

# Simulation and experiment of recycle micromixer with high reflux

Xiuhua He<sup>1</sup> ✉, Lingfeng Gao<sup>1</sup>, Yan Wang<sup>1</sup>, Benjamin B. Uzoejinwa<sup>1,2</sup>, Zhidan Deng<sup>3</sup>

<sup>1</sup>School of Energy and Power Engineering, Jiangsu University, Zhenjiang, Jiangsu, People's Republic of China

<sup>2</sup>Agricultural and Bioresources Engineering Department, University of Nigeria, Nsukka, Nigeria

<sup>3</sup>Faculty of Science, Jiangsu University, Zhenjiang, People's Republic of China

✉ E-mail: xiuhua.he@ujs.edu.cn

Published in Micro & Nano Letters; Received on 14th June 2017; Revised on 29th June 2017; Accepted on 10th July 2017

To overcome the low mixing efficiency near the vicinity of the wall of the micromixer, a passive micromixer using the recycle flow, with the advantages of simple structure, high reflux rate and high mixing efficiency, has been designed and investigated. In this work, the influence of different structural parameters and fluid properties on the mixing performance was studied by using commercial software ANSYS CFX. The mixing effect of micromixer was also studied by the experiments. A full comparison between the experimental results and simulation results was carried out. The numerical simulation results show that as the jet intensity increases and the viscosity of fluid becomes lower, the reflux rate and mixing efficiency of the micromixer are improved continuously; when Reynolds number (Re) is  $>15$ , the maximum reflux rate of the micromixer and the mixing efficiency exceed 35 and 95%. In addition, it was also observed that the simulation results are consistent with the experiments which revealed that the numerical simulation method applied and the results obtained in this work are reliable.

**1. Introduction:** Since the 1990s, Manz and Widmer first proposed the concept of 'micro total analysis system'. The microelectromechanical system (MEMS) has been developed in the direction of miniaturisation and integration of the equipment. The MEMS integrates the functions of preparation, mixing, separation, reaction and detection of the sample in the field of biology and chemistry, and controls the whole system through the fluid [1–3]. As an important part of MEMS, the micromixer is mainly used to achieve sufficient mixing of the different reactants under microscale conditions which have been widely used in micro-analytical chemistry, biochip and microchemical system [4].

Micromixer can be divided into active and passive ones according to the availability of additional power sources. The passive micromixer mainly uses microchannels with special geometrical structures to induce chaotic convection. So that it can increase the convection strength of the fluid and the mixing efficiency. The passive micromixer starts with the T-type and Y-type micromixers designed by Kamholz [5] and Ismagilov [6]. Now the micromixer has been developed into an important branch of microfluidics. Scholars have done a lot of researches and a number of new micromixers have been designed. The main types of passive micromixers include: the micromixer built-in baffle or block (He *et al.* [7], Chen and Zhao [8]), the type of chaotic convection (Stroock *et al.* [9], Hassell and Zimmerman [10]), the type of split and recombine (Viktorov *et al.* [11], Ansari and Ky [12]) and so on. As the Reynolds number (Re) of the mixed fluids in the micromixer is generally small, the fluids can only be mixed by molecular diffusion which caused the mixing performance near the contact surface of the two fluids more efficient. However, the fluid near the wall of the microchannel which has no contact is relatively inefficient. To overcome this shortcoming, some scholars have proposed the recycle micromixer which takes the fluids near the wall of the microchannel to the circulation channel and to re-mix. Jeon *et al.* [13] studied a recycle micromixer based on the conda effect. The results show that the backflow occurs in the circulation channel when  $Re = 12.9$ , and the mixing efficiency can be 94%. However, when the Re is  $<12.9$ , the mixing efficiency is relatively low. Zhang *et al.* [14] studied a recycle micromixer with high reflux rate. When  $Re = 85$ , the reflux rate is 20%, but the mixing efficiency is only 55%. The main channel of the two micromixers is bifurcated, which results in the complex structure and difficulty in processing.

To solve the above problems, this Letter presents a passive micromixer with a high return flow rate based on the principle of jet, which has the advantages of simple structure, favourable reflux generation and high mixing efficiency.

**2. Numerical simulation::** The scale of the micromixer is in the range of tens to hundreds of microns, much larger than the mean free path of the molecule, so that the fluid flowing in the microchannel can be regarded as an incompressible viscous fluid. The continuity equation, the incompressible fluid Navier–Stokes (N–S) equation and the convection-diffusion equation can be reduced to (1)–(3) under the no slip boundary condition

$$\nabla \cdot (\mathbf{u}) = 0 \quad (1)$$

$$\mathbf{u} \cdot \nabla \mathbf{u} = -\frac{1}{\rho} \nabla P + \nu \nabla^2 \mathbf{u} \quad (2)$$

$$D \nabla^2 c = \mathbf{u} \cdot \nabla c \quad (3)$$

where  $\mathbf{u}$ ,  $\rho$ ,  $P$ ,  $D$ ,  $\nu$  and  $C$ , respectively, represent the fluid velocity vector, fluid density, pressure, diffusion coefficient, kinematic viscosity and fluid concentration.

The mixing process of adiabatic, steady and incompressible fluid in the micromixer was simulated by ANSYS CFX. The continuity equation, the N–S equation and the convection-diffusion equation are used as control equations during numerical simulation without the energy equation, because no chemical reaction occurs in the mixing process. The SIMPLEX algorithm was used for pressure–velocity coupling. The inlet is set as the speed inlet, the outlet is set as the pressure outlet and the relative static pressure is set to zero.

The mass fraction of the two fluids to be mixed is set to 1 and 0, respectively, during the numerical simulation; keep the volume flow rate of the two fluids to be mixed consistent during the simulation in order to simplify the calculation. The Re of the flow in this study is in the range of 0.1–80, covering three different flow states: stratified flow, vortex flow and engulfment flow. Re is calculated by the physical parameters of the fluid to be mixed and the hydraulic diameter of the micromixer inlet, the formula is

$$Re = \rho v d / \nu \quad (4)$$

where  $\rho$  is the fluid density,  $v$  is the velocity of the fluid at the inlet,  $d$  is the hydraulic diameter of the micromixer at the inlet and  $\nu$  is the hydrodynamic viscosity.

The mixing efficiency is the key indicator of the performance of micromixers, which will directly affect the quality and quantity of various reactions. In order to quantitatively evaluate the degree of mixing of the micromixer, define the mixing efficiency as  $M$ , the calculation method is shown as follows:

$$M = \left( 1 - \frac{\int_0^{\omega} |C - C_{\infty}| dx}{\int_0^{\omega} |C_0 - C_{\infty}| dx} \right) \times 100\% \quad (5)$$

where  $C$  is the mass fraction of the fluid at the outlet of the micromixer;  $C_{\infty}$  is the mass fraction of the fluid when the mixing is complete ( $C_{\infty}=0.5$ );  $C_0$  represents the mass fraction of the fluid before the start of mixing;  $\omega$  represents the width of the outlet. According to the formula, the mixing efficiency  $M$  is in the range of 0–1, and the bigger the  $M$  is, the higher the mixing efficiency of the micromixer is;  $M=1$  means that the two media have been completely mixed, and  $M=0$  means that the two medias are not mixed at all [15].

In this Letter, the software, Gambit, is used to mesh the micromixer geometry model, and the grid type is unstructured hexahedral mesh. In order to improve the calculation speed under the premise of ensuring the reliability of results, the grid encryption is only taken for the key areas (such as jet nozzle, mixing area etc.), and the block coupling method is used to weaken the impact of the diffusion value of the simulation. When the number of grids is 405,300, 888,900 and 117.24 million, the maximum errors are 7.18, 4.52 and 0.56%, respectively, and the numerical simulation results of mixing efficiency are compared with the results with the number of grids of 2.0252 million. In order to improve the speed of numerical simulation, the total number of grid can be set as 1.172 million.

Fig. 1 shows the graphic structure of the micromixer, the dimension of the structure is in  $\mu\text{m}$ . The height of the micromixer and the width of the main channel are 200  $\mu\text{m}$ , and the angle formed by all the slanted lines and the centre line in the figure is 45°. Each circulation unit consists of a jet nozzle, a mixing zone, a mixture outlet and a set of symmetrical circulation channels. The micromixer is composed of four such circulation units, and the distance between each unit is 700  $\mu\text{m}$ .

**3. Experimental procedures:** In this experiment, the polydimethylsiloxane (PDMS) with high transparency and

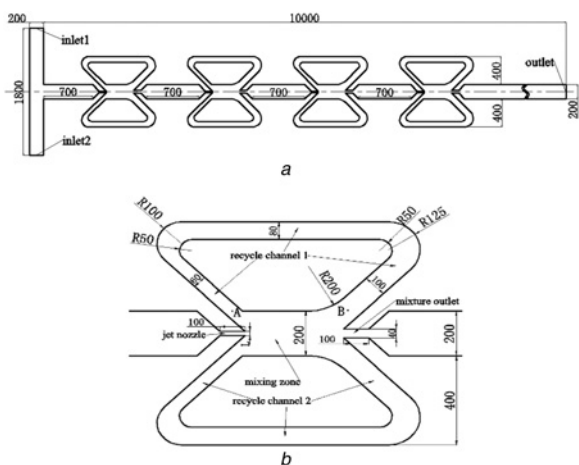


**Fig. 1** Graphic structure of the micromixer  
a Schematic diagram of the micromixer  
b Enlarged view of the micromixer

precision was used to fabricate the flow channels of the micromixer which makes it more clear to observe the flow characteristics of the fluids in the micromixer through a microscope. The cover plate of the micromixer is made of Pyrex with high hardness. The software CAD 2016 is used to draw the two-dimensional graphics. The mould of the micromixer is obtained by using silicon deep etching process according to the size of the channel. Then the liquid PDMS is poured into the moulds. The PDMS will be peeled off from the wafer mould to obtain the flow channels of the micromixer after the PDMS is completely cured. In this experiment, the technology of electrostatic bonding is used to combine the PDMS substrate with cover plate. Fig. 2 shows the micromixer which has already been made. In order to achieve the obvious effect in the mixing process, two reagents with different colour (black ink and deionised water) are used to make the mixed streamlines more visible.

To investigate the mixing performance of the micromixer with high reflux, an experiment was carried out and the experimental equipment was arranged as shown in Fig. 3. Two reagents were injected into the inlets by a syringe pump (Longer LSP02-1B). The flow state in the flow path was observed by an inverted microscope (Nikon ECLIPSE Ti-s). CCD camera (Nikon DIGITAL SIGHT DS-Ri1) was used to shoot the flow state diagram and import the diagram into a computer for comparison.

**4. Results and discussion:** This Letter compares the simulation results with the experiment results at  $Re=0.1, 0.7, 15$  and  $40$ . The effects of different flow rate on the micromixer are shown in Fig. 4. Under the same  $Re$ , the upper side is the hybrid cloud image obtained by the simulation, and the other side is the image obtained by the experiment.

To analyse the results of the experiments and simulations, the first step is to digitise the image information collected from the experiments. In this Letter, ImageJ was used to make the experimental photograph grey, and the results were put into the equation (6) to obtain the efficiency of the micromixer [16]

$$M = 1 - \frac{1}{I} \sqrt{\frac{1}{N} \sum_{i=1}^N (I_i - \bar{I})^2} \quad (6)$$

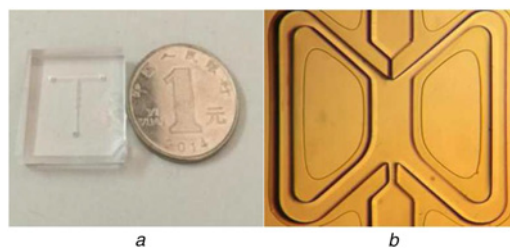


**Fig. 2** Physical picture of PDMS microfluidic chip  
a Comparison between PDMS microfluidic chip and coin  
b Enlarge view of the micromixer

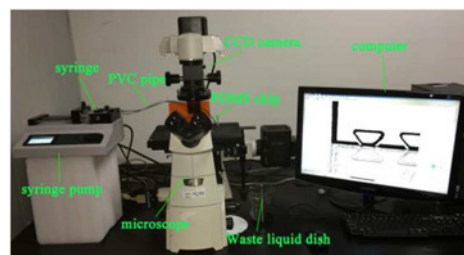


**Fig. 3** Experimental bench of PDMS microfluidic chip

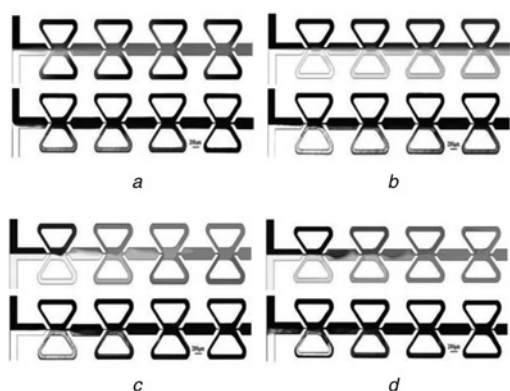


**Fig. 4** Comparison of concentration distribution between the simulation and experiment at various  $Re$

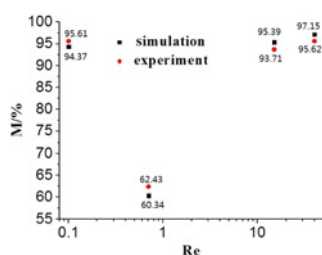
- a  $Re=0.1$
- b  $Re=0.7$
- c  $Re=15$
- d  $Re=40$

where  $N$  is the number of pixels in the measurement position,  $I_i$  is the grey value of a pixel at the measurement position ( $0 < I_i < 255$ ,  $\bar{I}$  represents the average of the grey values for all pixels

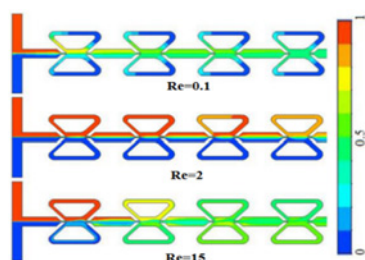
$$\bar{I} = \frac{1}{N} \sum_{i=1}^N I_i \quad (7)$$

Fig. 5 shows the comparison between the mixing efficiency of the numerical simulation and the experiments for  $Re=0.1, 0.7, 15$  and  $40$ . It can be seen from the figure that the error between the simulations and the experiments is very small, which proves the method of the numerical simulation used in this Letter is reliable and accurate.

Fig. 6 shows the concentration field at  $Re=0.1, 2$  and  $15$ . The mixing efficiency can be seen visually from the colour at the exit of the micromixer. When  $Re=0.1$ , due to the small flow rate, the mixing time of the mixed fluids is longer, the mixing efficiency



**Fig. 5** Comparison between mixing efficiency of experimental and simulation at different  $Re$



**Fig. 6** Concentration field of the micromixer at different  $Re$  (the red reagent represents the black ink and the blue reagent represents the deionised water)

is generally high. However in this case, the quantity of flow is too small (about  $3.875 \times 10^{-5}$  ml/s), which is difficult to achieve the requirements in practical application. When  $Re=2$ , the convection and molecular diffusion are both weak and laminar flow shows obviously, so the reverse pressure began to appear in the recirculation channel. Only a small amount of fluids began to return (the return rate was 0.68%). When  $Re=15$ , there was a large amount of fluids returned to the circulation channel (the return rate was 22.63%), and the reflux has become a major factor affecting the mixing efficiency. The reflux rate increases with the increase of the  $Re$  number. After several cycles of mixing, the fluid reaches a complete mix.

Fig. 7 shows the streamline of the mixed fluids at  $Re=2$  and  $15$  and from the left to the right are the mixing from start to the steady. The flow rate of the mixed fluids can be increased by the nozzle that in front of the mixing unit with the effect of jet, which makes the mixed fluids more prone to disturbance and changes the flow direction. When  $Re=2$ , due to the low flow rate, the streamline of the mixed fluids is almost distributed along the central plane symmetrically. When  $Re=15$ , the flow direction of the fluid is significantly deflected, so that the flow in the two recycle channels is different. Table 1 shows the distribution of the flow in the four mixing units at  $Re=2$  and  $15$ . When  $Re=2$ , the flow in the two recycle channels of each mixing unit is almost the same. However, when  $Re=15$ , there is a large difference in the flow between the two recycle channels of each mixing unit, which disturbs the mixed fluids more intense. By comparing Figs. 7a and b, the vortex is only generated near the outlet of the recycle channel and the strength of the vortex is small at  $Re=2$ , which makes it difficult to produce the turbulence in the mixed fluids, so the mixing efficiency of the micromixer is poor. When  $Re=15$ , due to the large difference in the flow between the two recycle channels, the mass flow rate of the backflow is very different, which produces a pair of vortices with different intensities in the mixing zone. Affected

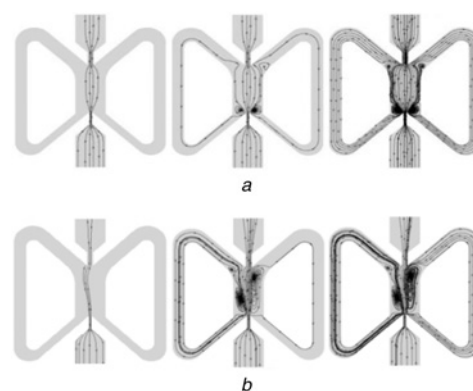


**Fig. 7** Streamlines of the first mixing unit of the micromixer at different  $Re$   
a  $Re=2$   
b  $Re=15$

**Table 1** Flow distribution in the circulation channel

		$Re=2$ , kg/s	$Re=15$ , kg/s
mixing unit 1	cycle channel 1	$2.645 \times 10^{-9}$	$8.476 \times 10^{-7}$
	cycle channel 2	$2.663 \times 10^{-9}$	$4.678 \times 10^{-7}$
mixing unit 2	cycle channel 1	$2.642 \times 10^{-9}$	$8.475 \times 10^{-7}$
	cycle channel 2	$2.659 \times 10^{-9}$	$4.678 \times 10^{-7}$
mixing unit 3	cycle channel 1	$2.639 \times 10^{-9}$	$8.465 \times 10^{-7}$
	cycle channel 2	$2.656 \times 10^{-9}$	$4.682 \times 10^{-7}$
mixing unit 4	cycle channel 1	$2.643 \times 10^{-9}$	$8.493 \times 10^{-7}$
	cycle channel 2	$2.655 \times 10^{-9}$	$4.673 \times 10^{-7}$

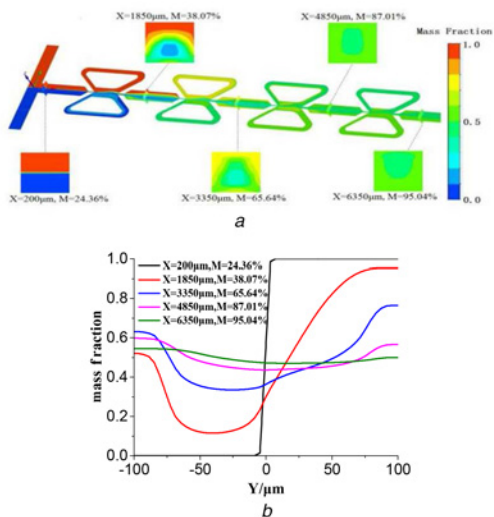


**Fig. 8** Concentration distribution at central surface and different cross-sections along  
 a Flowing direction at  $Re = 15$   
 b Mass fraction along the  $Y$ -axis at  $Re = 15$

by the two different vortices, the motion of the molecules becomes irregular, and the collision between the molecules is more intense, so that the mixing efficiency of the micromixer can be improved.

Fig. 8 shows the concentration of the centre plane and the cross-section at different locations along the flow direction of the micromixer at  $Re = 15$ . Fig. 8a shows that the interface between the samples becomes blurred and irregular with the increase of the mixing distance, because of the chaotic convection which was generated by the recycle channels stretches and cuts the mixed fluids continuously. Fig. 8b shows the variation of the mass fraction of the mixed fluids at the centre of the five sections in Fig. 8a in the  $Y$ -direction. Before entering the mixing unit, the mixed fluids can only be mixed by molecular diffusion, so its mixing efficiency is very low, only 24.36%. After the mixed fluids enter the mixing units, the flow rate is accelerated by the jet nozzle to form a pair of vortices. The vortices entrained the mixed fluids with low efficiency continuously, so that the flow and the pressure of the jet flow are increasing along the  $y$ -direction. When the mixed fluids reach the outlet of the mixing unit, its pressure is higher than the mixed fluids at the inlet of the same mixing unit. The mixed fluids with high mixing efficiency flows out directly from the outlet of the mixing unit, and the other part of the mixed fluids with lower efficiency enters the recycle channels under the influence of the pressure. After the mixed fluids passed through the four groups of recycle units, the highest mixing performance ( $M = 95.04\%$ ) has been achieved.

**5. Conclusion:** In this Letter, the influence of different structural parameters and fluid properties on the mixing performance of micromixer was studied by the numerical simulation and the experiments. We make a full comparison between the experimental results and simulation results. The experimental

results and the numerical simulation results keep a good consistency, which means that the numerical simulation method used in this Letter is reliable. In the mixing process, the jet in the mixing zone would always be deflected, resulting in a large difference in the amount of recycle flow between two circulation channels. This asymmetric recirculation makes the collision of fluid molecules more intense and chaotic convection much more stronger resulting in a high mixing efficiency.

**6. Acknowledgments:** This work was supported by the project of the National Natural Science Foundation of China (grant no. 51276082), Departments of Education and Finance, Jiangsu Province of PR China (A Project Funded by the Priority Academic Program Development of Jiangsu Higher Education institutions, PAPD) [grand no. SUZHENGBANFA (2014) No. 37].

## 7 References

- [1] Lin B.C., Qin J.H.: 'Graphic microfluidic lab-on-a-chip' (Science Press, Beijing, 2006)
- [2] Daw R.: 'Finkelstein J. Lab on a chip', *Nature*, 2006, **442**, (7101), pp. 367–367
- [3] Beebe D.J., Mensing G.A., Walker G.M.: 'Physics and applications of microfluidics in biology', *Annu. Rev. Biomed. Eng.*, 2002, **4**, pp. 261–286
- [4] He X., Wei D., Deng Z., *ET AL.*: 'Mixing performance of a novel passive micromixer with logarithmic spiral channel', *J. Drainage Irrigation Mach. Eng.*, 2014, **32**, (11), pp. 968–972
- [5] Kamholz A.E., Weigl B.H., Finlayson B.A., *ET AL.*: 'Quantitative analysis of molecular interactive in microfluidic channel: the T-sensor', *Anal. Chem.*, 1999, **71**, pp. 5340–5347
- [6] Ismagilov R.F., Stroock A.D., Kenis P.J.A., *ET AL.*: 'Experimental and theoretical scaling laws for transverse diffusive broadening in two-phase laminar flows in microchannels', *Appl. Phys. Lett.*, 2000, **76**, pp. 2376–2378
- [7] He X., Yan J., Wang Y.: 'T-shaped micromixer with periodic baffles', *Opt. Precis. Eng.*, 2015, **23**, (10), pp. 2877–2886
- [8] Chen X., Zhao Z.: 'Numerical investigation on layout optimization of obstacles in a three-dimensional passive micromixer', *Anal. Chim. Acta*, 2017, **1**, pp. 142–149
- [9] Stroock A.D., Dertinger S.K.W., Ajdari A., *ET AL.*: 'Chaotic mixer for microchannels', *Science*, 2002, **295**, pp. 647–651
- [10] Hassell D.G., Zimmerman W.B.: 'Investigation of the convective motion through a staggered herringbone micro-mixer at low Reynolds number flow', *Chem. Eng. Sci.*, 2006, **61**, pp. 2977–2985
- [11] Viktorov V., Mahmud M.R., Visconte C.: 'Design and characterization of a new H-C passive micromixer up to Reynolds number 100', *Chem. Eng. Res. Des.*, 2016, **108**, pp. 152–163
- [12] Ansari M.A., Ky K.: 'Mixing performance of unbalanced split and recombine micromixers with circular and rhombic sub-channels', *Chem. Eng. Sci.*, 2012, **76**, pp. 37–44
- [13] Jeon M.K., Kim J.H., Noh J., *ET AL.*: 'Design and characterization of a passive recycle micromixer', *J. Micromech. Microeng.*, 2005, **15**, pp. 346–350
- [14] Zhang D., Wang T., Gao Y., *ET AL.*: 'Design and numerical simulation of a high reflux passive micromixer', *Chin. J. Sens. Actuators*, 2013, **26**, (11), pp. 1621–1626
- [15] Hsieh S.S., Huang Y.C.: 'Passive mixing in micro-channels with geometric variations through  $\mu$ PIV and  $\mu$ LIF measurements', *J. Micromech. Microeng.*, 2008, **18**, (6), 065017
- [16] Lee Y.K., Tabeling P., Shih C., *ET AL.*: 'Characterization of a MEMS-fabricated mixing device', *Biochim. Biophys. Acta*, 2000, **157**, (3), pp. 558–565